Available online at www.sciencedirect.com
ScienceDirect
Theoretical Population Biology 71 (2007) 401–407
Theoretical Population Biology
www.elsevier.com/locate/tpb

Relating dispersal and range expansion of California sea otters

Martin Krkošek[a,*], Jean-Sébastien Lauzon-Guay[b], Mark A. Lewis[a]

[a]*Center for Mathematical Biology, Departments of Mathematical and Statistical Sciences and Biological Sciences, University of Alberta, Edmonton, Alberta, Canada T6E 2E7*
[b]*Department of Biology, University of New Brunswick, Fredericton, New Brunswick, Canada E3B 6E1*

Received 6 March 2006
Available online 21 February 2007

Abstract

Linking dispersal and range expansion of invasive species has long challenged theoretical and quantitative ecologists. Subtle differences in dispersal can yield large differences in geographic spread, with speeds ranging from constant to rapidly increasing. We developed a stage-structured integrodifference equation (IDE) model of the California sea otter range expansion that occurred between 1914 and 1986. The non-spatial model, a linear matrix population model, was coupled to a suite of candidate dispersal kernels to form stage-structured IDEs. Demographic and dispersal parameters were estimated independent of range expansion data. Using a single dispersal parameter, α, we examined how well these stage-structured IDEs related small scale demographic and dispersal processes with geographic population expansion. The parameter α was estimated by fitting the kernels to dispersal data and by fitting the IDE model to range expansion data. For all kernels, the α estimate from range expansion data fell within the 95% confidence intervals of the α estimate from dispersal data. The IDE models with exponentially bounded kernels predicted invasion velocities that were captured within the 95% confidence bounds on the observed northbound invasion velocity. However, the exponentially bounded kernels yielded range expansions that were in poor qualitative agreement with range expansion data. An IDE model with fat (exponentially unbounded) tails and accelerating spatial spread yielded the best qualitative match. This model explained 94% and 97% of the variation in northbound and southbound range expansions when fit to range expansion data. These otters may have been fat-tailed accelerating invaders or they may have followed a piece-wise linear spread first over kelp forests and then over sandy habitats. Further, habitat-specific dispersal data could resolve these explanations.

Keywords: Invasion; Dispersal; Spread rate; Matrix model; Dispersal kernel; Integrodifference equation; Sea otter

1. Introduction

Ecologists have long struggled to relate small scale dispersal and demographic processes with geographic population expansion, both for explaining and predicting the spread of invasive species. Demographic parameters often vary across life-history stages, with stage-specific survivorships, fecundities, and density dependencies. These differences can be captured by matrix population models when reproduction occurs seasonally or in discrete events (Caswell, 2001). Dispersal may also differ among life-history stages and this can be captured by stage-structured integrodifference equations (IDEs). These models couple a matrix population model with stage specific dispersal kernels that redistribute individuals in space according to the dispersal propensity specific to each population stage (Neubert and Caswell, 2000). In this way a detailed description of the dispersal behaviour and demography of a population can be captured in a single model.

Testing models of range expansion require independence between data used to estimate dispersal and demographic parameters and data used to test predictions of geographic range expansion. While traditional reaction–diffusion models have received many empirical tests (Lubina and Levin, 1988; Andow et al., 1990; Shigesada and Kawasaki, 1997; Ortega-Cejas et al., 2004), there are few examples where fat-tailed integrodifference models are tested (Schofield, 2002; Gilbert et al., 2004). This seems surprising, since many invasions are marked by non-linear or accelerating

*Corresponding author.
E-mail address: mkrkosek@ualberta.ca (M. Krkošek).

0040-5809/$ - see front matter © 2007 Elsevier Inc. All rights reserved.
doi:10.1016/j.tpb.2007.01.008

spatial spread (Shigesada and Kawasaki, 1997). We developed stage-structured IDE modes to relate dispersal and rang expansion of California sea otters (*Enhydra lutris nereis*). We examine how subtleties in dispersal scale to divergent patterns of geographic range expansion by comparing dispersal kernels that predict constant and accelerating invasion speeds. We then compare our results with those of Lubina and Levin (1988) and offer an alternate explanation for the observed patterns of spread—that otters may have been fat-tailed invaders.

1.1. Models of spread

The earliest models of population spread were reaction–diffusion equations of the type

$$\frac{\partial n}{\partial t} = rn + D\frac{\partial^2 n}{\partial x^2}, \tag{1}$$

which are the spatial counterparts of the exponential growth model $dn/dt = rn$, where r is the intrinsic rate of growth. The diffusion term, $D\partial^2 n/\partial x^2$, captures the spatial movement of individuals (Fisher, 1937; Skellam, 1951). This model assumes dispersal data are normally distributed, that individuals reproduce and disperse continually, and predicts that invading populations will spread at an asymptotically constant velocity

$$c = 2\sqrt{Dr} \tag{2}$$

(Skellam, 1951).

The discrete-time analog of the exponential growth model is $n_{t+1} = Rn_t$, where R is the net reproductive rate. To add spatial movements to this linear population growth model a dispersal kernel, $k(x-z)$, is introduced that defines the probability an individual will move from location z to location x in one time step. Since individuals can move from many locations, z, we must take the sum of all these possibilities. This yields a linear unstructured IDE of the form

$$n_{t+1}(x) = R\int_{-\infty}^{\infty} n_t(z)k(x-z)\,dz. \tag{3}$$

This model assumes discrete, non-overlapping generations with separate reproductive and dispersal phases (Kot et al., 1996). An advantage of IDEs is that they can utilize dispersal kernels of varying shapes. Thus, the assumption of normally distributed dispersal data underlying reaction–diffusion equations can be relaxed.

When the tails of the dispersal kernel are exponentially bounded, Eq. (3) yields an asymptotically constant invasion velocity

$$c = \min_{0<s<\hat{s}}\left[\frac{1}{s}\ln RM(s)\right], \tag{4}$$

which exists on the interval $0<s<\hat{s}$ and where $M(s)$ is the moment generating function of the kernel k defined on $[0,\hat{s})$ (Kot et al., 1996). When the dispersal kernel in Eq. (3) is the Gaussian with variance, θ^2, we recover Eq. (2) with $D = \frac{1}{2}\theta^2$ and $r = \ln(R)$ (Kot et al., 1996).

Differences in dispersal and demographic parameters across life-history stages can be captured by structuring the population. The non-spatial discrete-time model of this type is a linear matrix population model of the form $\mathbf{N}_t = \mathbf{A}\mathbf{N}_t$, where $\mathbf{N}$ is the vector of abundances (or densities) of life-history stages and $\mathbf{A}$ is the population projection matrix (Caswell, 2001). To add spatial movements of each population stage a redistribution matrix, $\mathbf{K}$, is used that has the same dimensions as $\mathbf{A}$ and is composed of stage-specific dispersal kernels that correspond to the stage transition elements in $\mathbf{A}$. Stage-structured IDEs have the form

$$\mathbf{N}_{t+1}(x) = \int_{-\infty}^{\infty}[\mathbf{A}\circ\mathbf{K}(x-z)]\mathbf{N}_t(z)\,dz, \tag{5}$$

(Neubert and Caswell, 2000). The symbol $\circ$ is the Hadamard product, and indicates element-by-element multiplication; each stage transition is coupled to its own unique dispersal kernel. A detailed derivation of Eq. (5) is given in Section 2 and also in Neubert and Caswell (2000). When all kernels in $\mathbf{K}$ have exponentially bounded tails, Eq. (5) yields constant invasion speeds given by

$$c = \min_{0<s<\hat{s}}\left[\frac{1}{s}\ln\rho_1(s)\right], \tag{6}$$

where $\rho_1(s)$ is the leading eigenvalue of the matrix $\mathbf{H}(s) = \mathbf{A}\circ\mathbf{M}(s)$, and $\mathbf{M}(s)$ is a matrix containing the moment generating functions of the kernels comprising $\mathbf{K}$ (Neubert and Caswell, 2000).

Leptokurtosis pervades most dispersal data. Leptokurtic dispersal kernels have more long-distance and short-distance dispersal events than would be seen with a Gaussian dispersal kernel with the same variance. Comparisons between leptokurtic and Gaussian dispersal kernels using unstructured IDEs have shown that the Gaussian assumption underestimates spread rates (Kot et al., 1996). Spread rates increase as the tails of the kernel become fatter, and in particular, Eq. (4) fails when the kernel has exponentially unbounded tails (Kot et al., 1996). These kernels are called fat tailed and they yield accelerating rates of spread. The same result holds when the IDE is stage structured and at least one stage transition disperses according to a fat-tailed kernel. In that case Eq. (6) fails and range expansion accelerates with time.

1.2. California sea otters

The California sea otter was hunted to near extinction in the early 1900s. In 1914 a remnant population of approximately 50 otters was discovered and protected, and then subsequently reinvaded its previous range. The population ceased expanding around 1982. Range expansion was well documented from 1938 onwards and those data and survey techniques are summarized in Lubina and Levin (1988).

Otters reproduce only once a year, typically in late winter or early spring. They have three distinct life-history stages: pups, juveniles, and adults. Pups, or newborn otters, are weaned after 6–8 months. The juvenile stage persists three to four years, after which individuals reach reproductive maturity. Otters inhabit near-shore habitats and aggregate in social groups of 4–40 individuals called rafts (Riedman and Estes, 1990).

Otter movement is characterized by sustained periods of localized movement punctuated by rare long-distance events (Ralls et al., 1996). Males disperse further than females, and juvenile males the farthest (Ralls et al., 1996). The population is spatially structured by age–sex classes: the outermost rafts are composed predominantly of juvenile males, whereas females occupy the central portion of the range (Riedman and Estes, 1990). For more information see Riedman and Estes (1990), Riedman et al. (1994), Ralls et al. (1996), Monnett and Rotterman (2000), and Laidre et al. (2001).

2. Model

We begin by constructing a linear stage-structured matrix population model, with three stages: pups (Y), juveniles (J), and adults (A). Then we add spatial movements by coupling each stage transition in the matrix model to a dispersal kernel that redistributes individuals in space for each time step. We do not include density dependencies in the population projection matrix since population density is low at the leading edge of the invasion wave. The validity of this approximation, relies on the linear conjecture (Mollison, 1991), which states that the asymptotic speed of invasion of the non-linear model is the same as at that of its linearization at low population density. It is expected to hold if there are no Allee effects and no long-distance density dependence (van den Bosch et al., 1990; Mollison, 1991). Allee effects were unlikely to slow the range expansion of sea otters since population expansion is limited by females (the reproductive unit) and there was an excess of males at the edges of the species range (Riedman and Estes, 1990).

The population vector is

$$\mathbf{N} = \begin{pmatrix} Y \\ J \\ A \end{pmatrix} \tag{7}$$

and the projection matrix is

$$\mathbf{A} = \begin{pmatrix} 0 & 0 & s_{aa}f \\ s_{yj} & s_{jj} & 0 \\ 0 & s_{ja} & s_{aa} \end{pmatrix} \tag{8}$$

which relates population size of each stage at time t to time $t+1$ by the matrix equation

$$\mathbf{N}_{t+1} = \mathbf{A}\mathbf{N}_t \tag{9}$$

(Caswell, 2001). Here, f is the average number of pups produced per adult otter per year, s_{yj} is the proportion of pups that survive to the juvenile stage each year, s_{jj} is the proportion of juveniles that survive to remain as a juvenile per year, s_{ja} is the proportion of juveniles that survive to become adults each year, and s_{aa} is the proportion of adults that survive each year.

The coastline can be modelled as an infinite one-dimensional homogenous habitat. It is appropriate for California sea otters since the scale of range expansion along the coast far exceeds the width of their nearshore habitat. That is, the sea otter population only expands along the coast, not out to sea. Habitat hererogeneities are not modelled, though they are undoubtedly important, since we are interested if knowledge of dispersal and demographic parameters alone is sufficient to account for population spread.

To incorporate spatial movements of otters we must track the movement of individuals through each stage of transition. The annual spatial movement of an individual can be modelled by a dispersal kernel, k, which defines the probability an individual will move a certain directional distance in a year. An individual located at z in year t will be found at location x at year $t+1$ with probability $k(x-z)$. For sea otters, the number of pups found in a subsequent year at location x that were produced by adults located at y is $fA_t(z)k_y(x-z)$. Since pups can arrive at location x from throughout the entire domain, the total number of pups arriving at location x must account for all sources z in the domain:

$$Y_{t+1}(x) = \int_{-\infty}^{\infty} fA_t(z)k_y(x-z)\,dz. \tag{10}$$

Similarly, the total number of juveniles and adults in a subsequent year at location x is

$$J_{t+1}(x) = \int_{-\infty}^{\infty} [s_{yj}Y_t(z)k_y(x-z) + s_{jj}J_t(z)k_j(x-z)]\,dz \tag{11}$$

and

$$A_{t+1}(x) = \int_{-\infty}^{\infty} [s_{ja}J_t(z)k_j(x-z) + s_{aa}A_t(z)k_a(x-z)]\,dz. \tag{12}$$

If we define the redistribution matrix, $\mathbf{K}$, as

$$\mathbf{K}(x) = \begin{pmatrix} k_y(x) & k_j(x) & k_a(x) \\ k_y(x) & k_j(x) & k_a(x) \\ k_y(x) & k_j(x) & k_a(x) \end{pmatrix}, \tag{13}$$

where k_y, k_j, and k_a are the stage specific dispersal kernels for pups, juveniles, and adults, respectively, we can write the stage-structured IDE that concisely captures all of the above information:

$$\mathbf{N}_{t+1}(x) = \int_{-\infty}^{\infty} [\mathbf{A} \circ \mathbf{K}(x-z)]\mathbf{N}_t(z)\,dz, \tag{14}$$

where $\circ$ is the Hadamard product that indicates element by element multiplication.

3. Parameter estimation and analysis

We calculated demographic parameters from the current literature, with estimates given in Table 1. Note that these estimates are independent of range expansion data. Dispersal kernels with exponentially bounded and unbounded tails were fit to annual dispersal data using maximum likelihood (Tables 2 and 3). Annual net displacements of otters were calculated from a long-term telemetry study of California sea otters (Ralls et al., 1996). Males were excluded since females are the limiting reproductive unit, and therefore the rate-limiting step in the invasion process. Juvenile and adult females were included together due to the small sample size (22 individuals). No data were available on pups so we assumed that pups do not disperse and approximated their movement by the delta function, $\delta(x)$. That is, pups remain in the same location with probability 1. Combining dispersal and demographic parameters into a stage structured IDE we have Eq. (14) as our model with

$$\mathbf{K}(x) = \begin{pmatrix} \delta(x) & k(x) & k(x) \\ \delta(x) & k(x) & k(x) \\ \delta(x) & k(x) & k(x) \end{pmatrix}. \tag{15}$$

After fitting each kernel we explored how well each model related dispersal and range expansion data. The dispersal parameter, α, was estimated directly from dispersal data and indirectly by fitting the full IDE solution to range expansion data. The IDE was solved numerically using a fast Fourier transform algorithm in Matlab. This allowed us to compare estimates of α and differences in kernel shapes between fits to dispersal data and range expansion data. Using maximum likelihood methods we could assess whether the estimate from range expansion data fell within the 95% confidence intervals of the dispersal estimate. In addition, we asked whether the predicted invasion velocities of models 1 and 2 (by Eq. (4)) were captured within the 95% confidence intervals of the observed invasion velocities. Finally, by comparing fits of the models to range expansion data, we could evaluate the capacity of each model to capture the pattern of spread observed in the range expansion data.

There are uncertainties in the initial population size in 1914 (Lubina and Levin, 1988). Therefore, with the dispersal kernels estimated by dispersal data, we left this as a free parameter (integer values only) and forced the solution to connect (as closely as possible) the source location in 1914 with the average distance between the northern and southern fronts in 1938 (the first reliable data). The remaining range expansion data then served as an independent test of how well each model performed. We used these same initial conditions to fit the models to range expansion data with α from the underlying kernel as a free parameter (Table 3).

Table 1
Sea otter demographic parameters

Parameter	Description	Value
f	Offspring per otter[a]	0.45
s_{yj}	Proportion of pups becoming juveniles per year[b]	0.60
s_{jj}	Proportion of juveniles remaining in juvenile stage per year[c]	0.631
s_{ja}	Proportion of juveniles becoming adults per year[c]	0.269
s_{aa}	Annual adult survivorship[d]	0.90

Survivorship values were taken from post-invasion studies and adjusted to account for the temporal length of each stage.
[a]Riedman et al. (1994).
[b]Monnett and Rotterman (2000).
[c]Eberhardt (1995).
[d]Siniff and Ralls (1991).

Table 2
Redistribution kernels fit to California sea otter dispersal data

Model	Spread rate	$k(x)$	L	L_3/L_j
1	Constant	$\frac{1}{\sqrt{2\pi\alpha^2}}\exp\left[\frac{-x^2}{2\alpha^2}\right]$	1.2398×10^{-31}	3.365×10^4
2	Constant	$\frac{1}{2\alpha}\exp\left[\frac{-\lvert x\rvert}{\alpha}\right]$	9.7010×10^{-30}	430
3	Accelerating	$\frac{1}{4\alpha}\exp\left[-\sqrt{\frac{\lvert x\rvert}{\alpha}}\right]$	4.1718×10^{-27}	1
4	Accelerating	$\frac{2\alpha}{\pi(\alpha^2+x^2)}$	8.0101×10^{-30}	520

Maximum likelihood was used to estimate the parameter, α, and likelihood ratios to compare fits among redistribution kernels to dispersal data (see also Table 3 and Fig. 1). Dispersal distances for 22 radio tagged female otters were calculated from Ralls et al. (1996).

Table 3
Estimates for the dispersal parameter, α, and the initial population size N_0

Model	Dispersal	North	South	Radius	N_0
1	8.49 (6.41, 12.00)	5.8	13.7	9.8	13
2	5.19 (3.45, 8.33)	4.1	9.8	7.0	13
3	0.71 (0.39, 1.35)	0.6	1.2	1.0	12
4	2.10 (0.89, 4.43)	0.3	1.2	1.1	19

The dispersal column shows the maximum likelihood estimates (±95% CI) by fitting the dispersal kernels to dispersal data. The north, south, and radius columns show the estimate for α from least-square regression of the numerical solution of the full IDE model to sea otter range expansion data. Radius is the range radius—the mean of the northern and southern expanding fronts. The N_0 column is the estimated initial population size by fitting the model parameterized by dispersal data through the starting point in 1914 and the average between northern and southern fronts in 1938 (the first reliable data).

4. Results

Parameter estimates of survivorship and fecundity for each sea otter stage were estimated from the literature

(Table 1). These estimates were used to parameterize a linear matrix model for sea otter population growth. The net reproductive rate can be calculated from the linear population projection matrix by finding the leading eigenvalue of **A** (Caswell, 2001). We calculated the net reproductive rate was $\lambda = 1.06$, which translates into an intrinsic rate of growth, $r = \ln(\lambda) = 0.058$.

There was a clear ranking of dispersal kernels fit to the dispersal data (Table 2): model 3 was statistically the best fit, while the Gaussian (model 1) was the poorest. In Fig. 1 we illustrate the relationship between dispersal and range expansion for each model. Differences in kernel shape among fits to dispersal and range expansion data ranged from slight deviations for model 3 to dramatic changes in shape for model 1. The shapes of the fat-tailed kernels (models 3 and 4) were well preserved across fits to dispersal and range expansion data. Estimates for α calculated from dispersal data and range expansion data were in close correspondence. When fit to range expansion data, all models yielded estimates for α, based on range radius, that were within the 95% confidence intervals of the observed α value (Table 3). Only model 3 yielded estimates for α from both northern and southern expanding fronts that fell within the 95% confidence intervals, while other models had one or no estimates from northern and southern expanding fronts that fell within these intervals.

Using Eq. (6), the predicted invasion speed from model 1 (containing the Gaussian kernel), was 2.75 km yr^{-1}, slightly greater than 2.41 km yr^{-1} predicted by model 2. The observed velocities of range expansion were calculated as the slope of the linear regression of range expansion vs. time data for the northern and southern fronts, excluding the initial data in 1914. Observed velocities were 2.63 km yr^{-1} (95%CI: 2.22, 3.03) for the north,

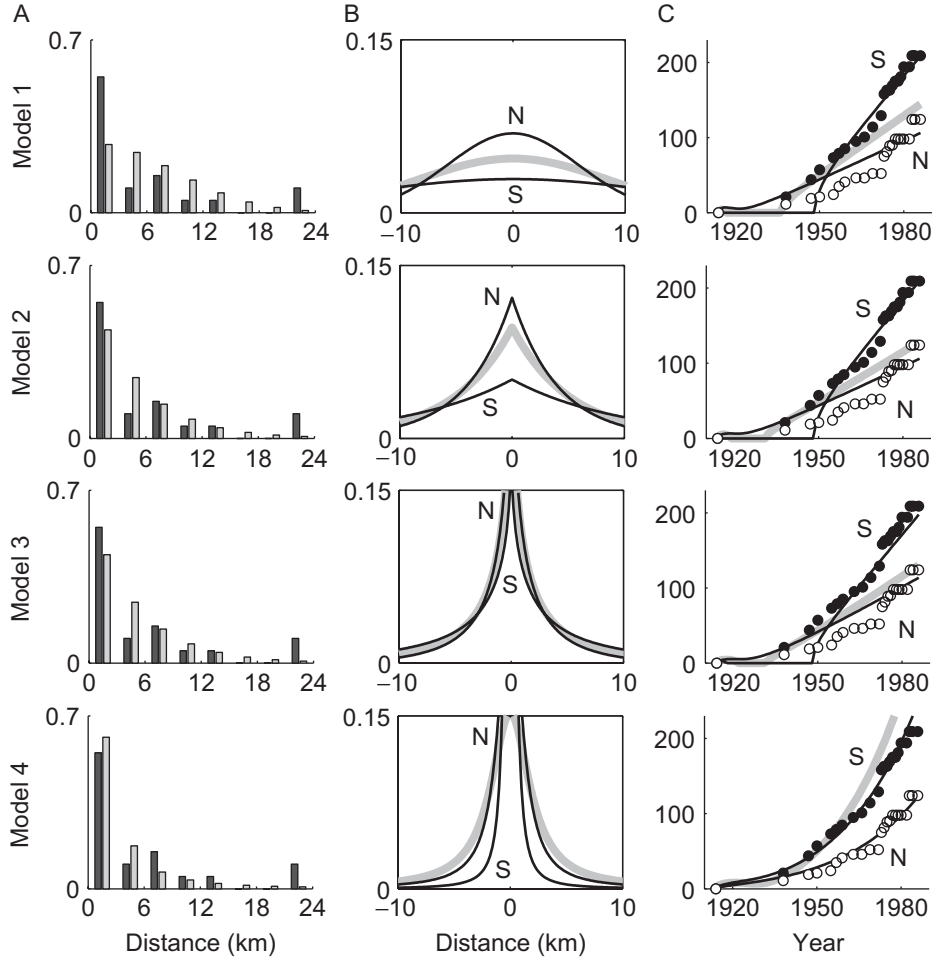

Fig. 1. The relationships between dispersal and range expansion for the California sea otter. Column (A) shows the frequency distributions of dispersal distances per juvenile and adult female otter per year (black bars) and the frequency distributions of the corresponding best-fit kernels given in Table 2 (grey bars) (distances were not binned in the maximum likelihood estimation). Column (C) shows the range expansion of otters moving south (filled circles) and north (open circles) in kilometers. Thick grey lines show the predicted range expansion based on numerical simulations of the sea otter integrodifference model with dispersal kernels from Table 2 and column (A). Thin black lines are the least-square best fits of the model to the southern and northern fronts, obtained by leaving α in the corresponding kernel as a free parameter. Column (B) shows the relationships among kernels fit from dispersal data (thick grey lines), the southern expanding front (thin black lines; S), and the northern expanding front (thin black lines; N). Simulations were conducted on a domain length of 1000 km with 32,768 grid points using a fast Fourier transform algorithm and detection threshold of 0.5 otters per kilometer.

4.35 km yr^{-1} (95%CI: 3.97, 4.74) for the south, and 3.49 km yr^{-1} (95% CI: 3.11, 3.87) for the range width. The predicted velocities of range expansion from both models 1 and 2 both fell within the 95% confidence limits for the northern expanding front, but not the southern front or the range width.

Although models 1 and 2 had good agreement between predicted and observed invasion velocities, these models were qualitatively lacking (Fig. 1). Models 1–3 showed a period of zero range width followed by sudden linear (or near linear) spatial spread. The period of zero range width occurred because the local population density fell below the detection threshold across the entire domain. However, the data show a more continuously accelerating invasion speed. Only model 4 was able to capture the accelerating nature of the sea otter invasion and adequately fit the entire range expansion data set. The fit of model 4 to range expansion data was excellent (north $R^2 = 0.94$, south $R^2 = 0.97$) and the predicted range expansion agreed well with the southern expanding front (Fig. 1). Overall, all models performed similarly in the quantitative tests despite the ranking of kernels by likelihood ratios. However, there was a clear accelerating feature in the range expansion data and models 1–3 failed to capture this. Only model 4 had a quantitative capacity to capture this feature and the predicted range expansion by model 4 captured this feature better than the other models.

5. Discussion

Relating dispersal and range expansion of invasive species remains one of the central challenges facing theoretical and quantitative ecologists. Small differences in dispersal can scale to large differences in geographic range expansion ranging from linear to accelerating spread rates (Kot et al., 1996). It follows that mathematical models used to predict and explain the spread of invasive species need to be tested to evaluate their utility and improve their predictive power. However, there are few data sets which have sufficient independence between small scale dispersal and demographic processes and geographic range expansion to allow such a test. With the recent publication of dispersal and demographic data for California sea otters we were able to meet the independence criteria and test a suit of invasion models in their ability to relate dispersal and range expansion. To our knowledge, this is the first rigorous empirical test of a suite of models that range in their predictions from linear to accelerating spread. All models were successful at predicting range expansion but there were subtleties in the quality of their predictions that correspond to uncertainty in dispersal data. There is a capacity for very high predictive power but this is challenged by the quantity and quality of dispersal data—especially in the tails of the distribution.

We began by deriving a linear matrix population model for California sea otters. From the population projection matrix we calculated the intrinsic rate of growth to be $r = 0.058$. This agrees well with estimates from Lubina and Levin (1988): $r = 0.056$ for California sea otters and $r = 0.054$ for Alaskan sea otters (calculated from the linear regression of log-transformed times series' of population abundances). The close correspondence of these estimates is encouraging—without considering any spatial data we have confidence in the demographic parameter estimates of the non-spatial matrix model. Thus, let us examine the spatial data—dispersal and range expansion—by focusing on a single parameter (α) that defines the shape of the dispersal kernel. By coupling a suit of dispersal kernels to the matrix model we formed a set of integrodifference models to relate dispersal and range expansion. Though similar, these models departed from each other in their predictions of range expansion—which ranged from linear to rapidly accelerating spread.

By fitting α to both dispersal and range expansion data we examined how well each model related small scale demographic and dispersal processes with emergent large scale population level patterns. There was a clear ranking of dispersal kernels by likelihood ratios, but, regardless, all models did a reasonable job of predicting the course of range expansion. Both models 1 and 2 predicted invasion velocities within the 95% confidence intervals of the observed spread rate of the northern moving front. All models estimated α from range radius data to be within the 95% confidence intervals of the α estimate from dispersal data. Only model 3 captured the estimated α from both northern and southern expanding fronts to be within the 95% confidence intervals, all other models captured either only one front or none. There was substantial variation among models in the qualitative agreement between predicted and observed range expansion. Only model 4 (the third ranked kernel) was able to capture the accelerating nature of the range expansion data. This model explained 94% and 97% of the variation in the range expansion data, indicating that this model had the capacity to predict range expansion with high accuracy. However, this model did not rank high when fit to dispersal data. Thus, the ranking of models by dispersal data and range expansion data do not correspond. This highlights the challenges facing ecologists when using these models as predictive tools but also highlights their capacity to provide interesting insights into mechanisms underlying patterns of invasive spread—such as non-linearities.

The range expansion data reveal an interesting non-linear feature: range expansion was initially slow and then rapidly accelerated. Our results suggest that this can be explained with a model of dispersal that allows for a relatively high frequency of long-distance dispersers. This model, model 4, has a dispersal kernel with exponentially unbounded tails and predicts an accelerating rate of spread that matches nearly exactly the observed pattern of spread. This suggests that long-distance dispersal may have driven this non-linear feature in sea otter spread. Accelerating spread could be also be produced by an Allee effect but we think this is not the case for sea otters. Males dominate the outer limits of the population but females drive the

population expansion through reproduction. Because of this it is unlikely that females would have difficulty finding mates or be more susceptible to predation at the edge of their range. An alternative explanation for non-linear range expansion was proposed by Lubina and Levin (1988) in their analysis of the same range expansion data. Although they lacked the independence between dispersal and range expansion data that we enjoy, they achieved excellent piece-wise linear fits of a reaction–diffusion model to the California sea otter spread. They argued that range expansion was initially slow (but constant), corresponding to reduced dispersal behaviour in kelp forest habitats and then suddenly switched to fast (but still constant) dispersal over sandy bottom habitats. We did not consider habitat heterogeneities in our model since we were interested if knowledge of dispersal data alone was sufficient to account for the observed patterns of spread. Both explanations seem possible and could easily be resolved if detailed habitat-specific dispersal data became available.

Acknowledgments

This work started as a team project at a PIMS (Pacific Institute for the Mathematical Sciences) funded mathematical biology summer school for undergraduates at the University of Alberta. JSLG thanks M. Barbeau and J. Watmough for supporting his participation in the summer school. MK was supported by an NSERC Industrial Postgraduate Scholarship I and an NSERC Canada Graduate Scholarship D. JSLG was supported by an NSERC Post Graduate Scholarship. MAL was supported by NSERC Discovery and CRO grants and a Canada Research Chair.

References

Andow, D., Kareiva, P., Levin, S., Okubo, A., 1990. Spread of invading organisms. Landscape Ecol. 4, 177–188.

Caswell, H., 2001. Matrix Population Models. Sinauer, MA, USA.

Eberhardt, L., 1995. Using the Lotka–Leslie model for sea otters. J. Wildl. Manage. 59, 222–227.

Fisher, R., 1937. The wave of advance of advantageous genes. Ann. Eugen. 7, 353–369.

Gilbert, M., Gregoire, J., Freise, J., Heitland W., 2004. Long-distance dispersal and human population density allow the prediction of invasive patterns in the horse chestnut leafminer *Cameraria ohridella*. J. Anim. Ecol. 73, 459–468.

Kot, M., Lewis, M., van den Driessche, P., 1996. Dispersal data and the spread of invading organisms. Ecology 77, 2027–2042.

Laidre, K., Jameson, R., Demaster, D., 2001. An estimation of carrying capacity for sea otters along the California coast. Mar. Mamm. Sci. 17, 294–309.

Lubina, J., Levin, S., 1988. The spread of a reinvading species: range expansion in the California sea otter. Am. Nat. 131, 526–543.

Mollison, D., 1991. Dependence of epidemic and population velocities on basic parameters. Math. Biosci. 107, 255–287.

Monnett, C., Rotterman, L., 2000. Survival rates of sea otter pups in Alaska and California. Mar. Mamm. Sci. 16, 794–810.

Neubert, M., Caswell, H., 2000. Demography and dispersal: calculation and sensitivity analysis of invasion speed for structured populations. Ecology 81, 1613–1628.

Ortega-Cejas, V., Fort, J., Mendez, V., 2004. The role of the delay time in the modeling of biological range expansions. Ecology 85, 258–264.

Ralls, K., Eagle, T., Siniff, D., 1996. Movement and spatial use patterns of California sea otters. Can. J. Zool. Rev. Can. Zool. 74, 1841–1849.

Riedman, M., Estes, J., 1990. The sea otter (*Enhydra lutris*): behavior, ecology, and natural history. US Fish and Wildlife Service Biological Report 14, 126pp.

Riedman, M., Estes, J., Staedler, M., Giles, A., Carlson, D., 1994. Breeding patterns and reproductive success of California sea otters. J. Wildl. Manage. 58, 391–399.

Schofield, P., 2002. Spatially explicit models of Turelli–Hoffmann Wolbachia invasive wave fronts. J. Theor. Biol. 215, 121–131.

Shigesada, N., Kawasaki, K., 1997. Biological Invasions: Theory and Practice. Oxford University Press, Oxford, UK.

Siniff, D.B., Ralls, K., 1991. Reproduction, survival and tag loss in California sea otters. Mar. Mamm. Sci. 7, 211–229.

Skellam, J., 1951. Random dispersal in theoretical populations. Biometrika 38, 196–218.

van den Bosch, F., Metz, J., Diekmann, O., 1990. The velocity of spatial population expansion. J. Math. Biol. 28, 529–565.